Genetic structure of invasive baby's breath (*Gypsophila paniculata*) populations in a freshwater Michigan dune system

Hailee B. Leimbach – Maus[1,2], Syndell R. Parks[1], and Charlyn G. Partridge[1]

[1]Annis Water Resources Institute, Grand Valley State University (AWRI-GVSU), 740 W. Shoreline Dr., Muskegon, MI 49441 USA

[2]Corresponding author: Hailee B. Leimbach – Maus
Annis Water Resources Institute, Grand Valley State University (AWRI-GVSU)
740 W. Shoreline Dr., Muskegon, MI 49441 USA
Telephone: (440) 488-8042 (no fax)
Email addresses: hailee.leimbachmaus@gmail.com

Running title: Leimbach – Maus et al. – invasive baby's breath population structure

Word count: 6715.

ABSTRACT

Coastal sand dunes are dynamic ecosystems with elevated levels of disturbance, and as such they are highly susceptible to plant invasions. One such invasion that is of major concern to the Great Lakes dune systems is that of perennial baby's breath (*Gypsophila paniculata*). The invasion of baby's breath negatively impacts native species such as the federal threatened Pitcher's thistle (*Cirsium pitcheri*) that occupy the open sand habitat of the Michigan dune system. Our research goals were to (1) quantify the genetic diversity of invasive baby's breath populations in the Michigan dune system, and (2) estimate the genetic structure of these invasive populations. We analyzed 12 populations at 14 nuclear and 2 chloroplast microsatellite loci. We found strong genetic structure among populations of baby's breath sampled along Michigan's dunes (global $F_{ST} = 0.228$), and also among two geographic regions that are separated by the Leelanau peninsula. Pairwise comparisons using the nSSR data among all 12 populations yielded significant F_{ST} values. Results from a Bayesian clustering analysis suggest two main population clusters. Isolation by distance was found over all 12 populations ($R = 0.755$, $P < 0.001$) and when only cluster 2 populations were included ($R = 0.523$, $P = 0.030$); populations within cluster 1 revealed no significant relationship ($R = 0.205$, $P = 0.494$). Private nSSR alleles and cpSSR haplotypes within each cluster suggest the possibility of at least two separate introduction events to Michigan.

Key words: Invasive species, genetic diversity, genetic structure, invasion history, microsatellites, *Gypsophila paniculata*.

52

53 ## INTRODUCTION

54 Coastal sand dunes are dynamic ecosystems. Both the topography and biological community are
55 shaped by disturbance from fluctuations in water levels, weather patterns, and storm events
56 (Arbogast and Loope 1999, Everard et al. 2010, Blumer et al. 2012). In these primary
57 successional systems, vegetation plays an imperative role in trapping sand and soil, both of
58 which accumulate over time and result in sand stabilization and dune formation (Cowles 1899,
59 Olson 1958, Arbogast 2015). Much of the vegetative community native to coastal dune systems
60 is adapted to the harsh conditions posed by the adjacent coast, and some species require early
61 successional, open habitat to thrive (Albert 2000, Everard et al. 2010). For example, dune species
62 such as Marram grass (*Ammophila brevigulata*), Lake Huron tansy (*Tanacetum huronense*), and
63 Pitcher's thistle (*Cirsium pitcheri*) are adapted to sand burial and will continue to grow above the
64 sand height as it accumulates (Albert 2000). It is the heterogeneous topography and successional
65 processes due to continuous disturbance that makes dune systems so unique (Everard et al.
66 2010).

67 Because coastal dune ecosystems have naturally elevated levels of disturbance, they are
68 highly susceptible to plant invasions (Jorgensen and Kollman 2009, Carranza et al. 2010, Rand et
69 al. 2015). Invasive plant species are known to be adept at colonizing disturbed areas, and in
70 sparsely-vegetated dune systems that are often in early stages of succession, the opportunities for
71 invasive colonizers are great (Cowles 1899, Grime 1979, Baker 1986, Sakai et al. 2001). Coastal
72 dune systems also typically have a gradient of increasing stages of succession (Cusseddu et al.
73 2016) and this heterogeneous structure can further promote various stages of an invasion, such as
74 colonization, dispersal, and range expansion (With 2002, Theoharides and Dukes 2007).

Within the MI dunes system, these successional processes have resulted in a patchwork pattern with alternating areas of open dune habitat, interdunal swales, shrub-scrub, and forested pockets scattered across the landscape (Cowles 1899, Albert 2000, Blumer et al. 2012). This landscape structure can play an important role in shaping species migration, invasive spread, and population demographics (With 2002, Theoharides and Dukes 2007, Jorgensen and Kollman 2009), thus potentially driving patterns of population structure for invasive species. However, management of dune communities can also have a strong impact on invasive populations, as well as the native plant community and the landscape they are invading. Invasive beach grasses *Ammophila breviligulata* and *A. arenaria,* and the management practices used to reduce their impact, led to changes in the morphology of the coastal dune ecosystem by decreasing the maximum dune elevation (Zarnetske et al. 2010). Thus, just as a landscape can shape invasive populations, a plant invasion can also significantly alter the dune landscape (Grime 1979, Cowles 1899, Sakai et al. 2001, Zarnetske et al. 2010).

In addition to the landscape, demographic processes during a species' invasion also shape the genetic structure observed in contemporary populations. Multiple separate introduction events can result in contemporary populations that are genetically distinct from one another and from the native range (Dlugosch and Parker 2008, Crosby et al. 2014, Hagenblad et al. 2015). Bottleneck events during an introduction can further limit the genetic variation in the invasive range, though this has not necessarily been found to limit the success of an invader (Dlugosch and Parker 2008, Xu et al. 2015). Additionally, genetic admixture and inbreeding can shape the structure of populations, and the effect of these processes can be further influenced by the landscape structure and habitat heterogeneity (Crosby et al. 2014, Nagy and Korpelainen 2014, Moran et al. 2017, Bustamante et al. 2018).

Perennial baby's breath (*Gypsophila paniculata*) has been identified as a species of concern due to its impact on the integrity of the Michigan dune system (DNR 2015). A perennial iteroparous forb native to the Eurasian steppe region (Darwent and Coupland 1966, Darwent 1975), baby's breath has been found to negatively impact the coastal dune community in Michigan by crowding out sensitive species such as Pitcher's thistle (*Cirsium pitcheri*) through direct competition for limited resources, forming monotypic stands in the open dune habitat, preventing the reestablishment of native species, and limiting pollinator visits to native species (Baskett et al. 2011, Jolls et al. 2015, Emery and Doran 2013). Baby's breath dispersal is thought to be primarily wind-driven (Darwent and Coupland 1966), which is also the mechanism that shapes the dunes. Following seed maturity, the stems of baby's breath individuals become dry and brittle, breaking at the caudex and forming tumbleweed masses that can disperse roughly 10 000 seeds per plant up to 1 km (Darwent and Coupland 1966, Darwent 1975). Due to the topography and the heterogeneous habitat of the dune systems, the wind patterns of this landscape have the potential to shape the structure of invasive baby's breath populations. Wind can drive the direction and distance that baby's breath tumbleweeds disperse, and it is possible that wind patterns could both promote gene flow or limit it by driving tumbleweeds into undesirable habitat. Additionally, the steep topography in parts of the dunes could further prevent tumbleweeds from dispersing significant distances. With these interactive processes in mind, this study explored the genetic structure of invasive populations of baby's breath within the Michigan coastal dune system. The goals of this research were to (1) quantify the genetic diversity of invasive baby's breath populations in the Michigan dune system, and (2) estimate the genetic structure of these invasive populations. By estimating the genetic diversity and structure

120 of these invasive populations, we can better understand the impact the dune landscape and its
121 dynamic processes have on this plant invasion.
122
123 **METHODS**
124 **Study area and sample collection**
125 To determine the population structure of baby's breath on a regional scale in Michigan, we
126 collected leaf tissue from plants at 12 different sites in the summers of 2016-2017. All sites were
127 located in areas of known infestation along the dune system of Michigan (Figure 1), and the
128 majority have a history of treatment primarily by The Nature Conservancy, the Grand Traverse
129 Regional Land Conservancy, and the National Park Service (TNC 2013). Eleven sites were
130 located along Lake Michigan in the northwest lower peninsula of Michigan, and one was located
131 on Lake Superior in the upper peninsula. Seven of these sites are located within Sleeping Bear
132 Dunes National Lakeshore (hereafter Sleeping Bear Dunes or SBDNL), which contains one of
133 the largest infestations within the region. We collected leaf tissue samples (5-10 leaves per
134 individual) from a minimum of 20 individuals per site (maximum of 35), and stored them in
135 individual coin envelopes in silica gel until DNA extractions took place (total $n = 313$). Site
136 locations in Michigan (Supplemental A) were separated by a minimum of 10 km and a maximum
137 of 202 km. We subjectively chose individuals to be sampled by identifying a visibly infested
138 area, selecting individuals regardless of size, and walking a minimum of ca. 5 meters in any
139 direction before choosing another plant to minimize the chance of sampling closely related
140 individuals. We observed that the population distributions at the Petoskey State Park and Grand
141 Marais sites were smaller and patchier than the others (ca. 60 individuals total), so we conducted
142 sampling more opportunistically. This opportunistic sampling involved collecting tissue from

143 individuals that were less than 5 m apart, and in some areas sampling from all individuals (ca. 3
144 – 4 individuals) within a small patch (ca. 5m x 5m).
145
146 **Microsatellite genotyping**
147 We extracted genomic DNA from all samples using DNeasy plant mini kits (QIAGEN, Hilden,
148 Germany) and followed supplier's instructions with minor modifications, including an extra
149 wash step with AW2 buffer. We then ran the extracted DNA twice through Zymo OneStep PCR
150 Inhibitor Removal Columns (Zymo, Irvine, CA) and quantified the concentrations on a
151 Nanodrop 2000 (Waltham, Massachusetts, USA). We included deionized water controls in each
152 extraction as a quality control for contamination.
153 We amplified samples at 14 polymorphic nuclear microsatellite loci (hereafter nSSRs)
154 that were developed specifically for *G. paniculata* using Illumina sequencing technology (Table
155 1) (Leimbach-Maus et al. 2018). We conducted polymerase chain reactions (PCR) using a
156 forward primer with a 5'-fluorescent labeled dye (6-FAM, VIC, NED, or PET) (Applied
157 Biosystems, Foster City, CA) and an unlabeled reverse primer. PCR reactions consisted of 1x
158 KCl buffer, 2.0-2.5 mM $MgCl_2$ depending on the locus (Table 1), 300 µM dNTP, 0.08 mg/mL
159 BSA, 0.4 µM forward primer fluorescently labeled with either FAM, VIC, NED, or PET, 0.4 µM
160 reverse primer, 0.25 units of Taq polymerase, and a minimum of 50 ng DNA template, all in a
161 10.0 µL reaction volume. The thermal cycle profile consisted of denaturation at 94˚C for 5
162 minutes followed by 35 cycles of 94˚C for 1 minute, annealing at 62˚C for 1 min, extension at
163 72˚C for 1 min, and a final elongation step of 72˚C for 10 minutes.
164 Each sample was also amplified at 2 universal chloroplast microsatellite loci (hereafter
165 cpSSRs) previously developed for *Nicotiana tabacum* L. (Chung and Staub 2003) (ccssr4,

ccssr9) (Table 1). PCR reactions were conducted using a forward primer with a 5'-fluorescent labeled dye and an unlabeled reverse primer. PCR reactions for the cpSSRs are the same as detailed above for the nuclear loci. The thermal cycler profile for cpSSRs is as follows: denaturation at 94˚C for 5 minutes followed by 30 cycles of 94˚C for 1 minute, annealing at 52˚C for 1 minute, extension at 72˚C for 1 minute, and a final elongation step of 72˚C for 8 minutes (modified from Calistri et al. 2014).

We determined successful amplification by visualizing the amplicons on a 2% agarose gel stained with ethidium bromide. We multiplexed PCR amplicons according to dye color and allele size range (Table 1), added LIZ Genescan 500 size standard, denatured with Hi-Di Formamide at 94˚C for four minutes, and then performed fragment analysis on an ABI3130xl Genetic Analyzer (Applied Biosystems) following instrument protocols. We genotyped individuals using the automatic binning procedure on Genemapper v5 (Applied Biosystems), and constructed bins following the Genemapper default settings. To account for the risk of genotyping error when relying on an automated allele-calling procedure, we visually verified that all individuals at all loci were correctly binned to minimize errors caused by stuttering, low heterozygote peak height ratios, and split peaks (DeWoody et al. 2006, Guichoux et al. 2011).

Quality control

Prior to any analysis, we used multiple approaches to check for scoring errors (DeWoody et al. 2006). We checked nSSR genotypes for null alleles and potential scoring errors due to stuttering and large allele dropout using the software Micro-Checker v2.2.3 (Van Oosterhout et al. 2004, Van Oosterhout et al. 2006). Prior to marker selection, the loci used in this study were previously checked for linkage disequilibrium (Leimbach-Maus et al. 2018). We checked for heterozygote

deficiencies in the package STRATAG in the R statistical program. We then screened our data for individuals with more than 20% missing loci and for loci with more than 10% missing individuals (Gomes et al. 1999, Archer et al. 2016). We found none, so all individuals and loci remained for further analyses. In addition, we genotyped 95 individuals twice to ensure consistent allele calls. For the nSSR dataset, we used Genepop 4.2 (Raymond and Rousset 1995, Rousset 2008) to perform an exact test of Hardy-Weinberg Equilibrium (HWE) with 1,000 batches of 1,000 Markov Chain Monte Carlo iterations (Gomes et al. 1999). We also checked for loci out of HWE in more than 60% of the populations; however, there were none.

nSSR genetic diversity

We calculated the total number of alleles per sampling location, private alleles, observed and expected heterozygosity in GenAlEx 6.502 (Peakall and Smouse 2006, 2012), and estimated the inbreeding coefficient (F_{IS}) in Genepop 4.2 (Raymond and Rousset 1995, Rousset 2008). We used the package diverSity in the R statistical program to calculate the allelic richness at each sampling location (Keenan et al. 2013).

nSSR genetic structure

To test for genetic differentiation between all pairs of sampling locations, we calculated Weir and Cockerham's (1984) pairwise F_{ST} values for 9,999 permutations in GenAlEx 6.502 (Peakall and Smouse 2006, 2012). In the R statistical program, we corrected the p-values using a false discovery rate (FDR) correction (Benjamini and Hochberg 1995). To test how much of the genetic variance can be explained by within and between population variation, we ran an

analysis of molecular variance (AMOVA) for 9,999 permutations in GenAlEx 6.502 (Peakall and Smouse 2006, 2012).

To examine the number of genetic clusters among our sampling locations, we used the Bayesian clustering program STRUCTURE v2.3.2 (Pritchard et al. 2000). Individuals were clustered assuming the admixture model both with and without a priori sampling locations for a burn-in length of 100,000 before 1,000,000 repetitions of MCMC for 10 iterations at each value of K (1 – 16). The default settings were used for all other parameters. We identified the most likely value of K using the Ln Pr(X|K) from the STRUCTURE output and the ΔK method from Evanno et al. (2005) in CLUMPAK (Kopelman et al. 2015).

To further explore the genetic structure of these populations, we ran a Principal Coordinates Analysis (PCoA) in GenAlEx 6.50, where the analysis was based on an individual pairwise genotypic distance matrix (Peakall et al. 1995, Smouse and Peakall 1999). To find and describe finer genetic structuring of the nSSR dataset, we performed a discriminant analysis of principal components (DAPC) in the R package *adegenet*, which optimizes among-group variance and minimizes within-group variance (Jombart 2008, Jombart et al. 2010). To identify the number of clusters for the analysis, a Bayesian clustering algorithm was run for values of K clusters (1 – 16). We retained a K-value of 3 based on the resulting Bayesian Information Criterion for each K-value and the results of the previously run PCoA that suggested 3 clusters may exist within the nSSR data. DAPC can be beneficial, as it can limit the number of principal components (PCs) used in the analysis. It has been shown that retaining too many PCs can lead to over-fitting and instability in the membership probabilities returned by the method (Jombart et al. 2010). Therefore, we performed the cross-validation function to identify the optimal number of PCs to retain. Out of 69 total PCs, the cross-validation function suggested we retain 60 PCs

(Jombart et al. 2010). We ran the DAPC using the recommended 60 PCs, but also checked if the general patterns remained with fewer PCs used by running the analysis with incrementally less PCs (45 and 30 PCs). All general patterns of the data in the scatterplots remained consistent despite the decreased PCs; therefore, we chose to use the scatterplot based on 30 PCs, as the benefit of the DAPC for our purposes is to show that the main patterns remain, despite minimization of within population variation (Jombart et al. 2010).

To assess the effect of isolation by distance (IBD), we used a paired Mantel test based on a distance matrix of Slatkin's transformed F_{ST} ($D = F_{ST}/(1 - F_{ST})$) (Slatkin 1995) and a geographic distance matrix for 9,999 permutations in GenAlEx 6.502, and the analysis follows Smouse et al. (1986) and Smouse and Long (1992). The mean geographic center was generated for each sampling location in ArcGIS software (ESRI^{TM} 10.4.1, Redlands, CA), and the latitude and longitude of these points was then used to construct a matrix of straight line distances in km between each sampling location. The reported p-values are based on a one-sided alternative hypothesis (H_1: $R > 0$). A Mantel test was run for all sampling locations together, and a test was also run separately for populations within each cluster identified in the STRUCTURE analysis.

cpSSR genetic diversity

For the cpSSR dataset, we used the program HAPLOTYPE ANALYSIS v1.05 (Eliades and Eliades 2009) to calculate the number of haplotypes, haplotype richness, private haplotypes, and haploid diversity. To visualize patterns in the cpSSR dataset, we created a minimum spanning network in the R package poppr (Kamvar et al. 2014). Nei's genetic distance was used as the basis for the network with a random seed of 9,999.

nSSR and cpSSR genetic structure

In order to compare the population structure of the nSSR and cpSSR data, we used the Φ_{ST} distance matrix for both datasets and ran an AMOVA. The population pairwise Φ_{ST} matrix facilitates comparison of molecular variance between codominant and dominant data by suppressing within individual variation, thus allowing for the comparison between varying mutation rates (Weir and Cockerham 1984, Excoffier et al. 1992). To test how much genetic variation could be explained by within populations, between populations, and between regions (genetic clusters identified through STRUCTURE analysis) for both datasets, we ran an AMOVA for 9,999 permutations in GenAlEx 6.502 (Peakall and Smouse 2006, 2012).

RESULTS

Microsatellite genotyping and genetic diversity

We genotyped 313 individuals from 12 locations at 14 nSSR loci (Table 1). No loci showed evidence for null alleles across all populations, there were no loci with more than 4 populations significantly out of HWE (less than 30% of populations) (Table 2), and no loci significantly deviated from linkage equilibrium across all populations. The nSSR loci were moderately polymorphic, and the number of alleles per locus per population ranged from 1 – 11, with a total of 85 alleles across 14 loci. Allelic richness (A_R) ranged from 2.32 – 4.21 per population with a mean of 3.53, and GM, PS, and TC populations exhibited lower levels of A_R than the other populations. Of the 6 private nSSR alleles identified, 5 were at low frequencies – occurring in five or fewer individuals, but the private nSSR allele in the GM population occurred in over 60% of individuals. Overall, the observed heterozygosity (H_O) averaged over loci for each population ranged from 0.25 – 0.56 with a mean of 0.46, and the 3 northernmost populations (GM, PS, TC)

had lower diversity in general. Expected heterozygosity (H_E) ranged from 0.30 – 0.57 across populations, with a mean of 0.49. GM and AD populations deviated significantly from HWE ($P < 0.05$). GM had a higher inbreeding coefficient (Table 2), but this could be attributed to our limited area in which to sample.

Both cpSSR loci were polymorphic, with 3 alleles per locus for a total of 6 alleles, and the number of alleles per population ranged from 2 – 4 with an average of 2.50 (Table 2). All alleles together resulted in 5 haplotypes. There were between 1 – 3 haplotypes per population for a haplotype richness ranging from 0.00 – 2.00, with a mean of 0.41 per population. Haploid diversity ranged from 0.00 – 0.58 with a mean of 0.10 per population. One allele and haplotype 2 were both unique to the SB and ZP sampling locations, and another allele and haplotype 4 were both private to five individuals sampled in GM, which occurred in a separate sampling location from the rest of the individuals in GM (Figure 5).

Genetic structure

The nSSR data suggested that there is strong genetic structure among the populations and regions of baby's breath sampled along the dunes of western and northern Michigan (global $F_{ST} = 0.228$). Pairwise comparisons using the nSSR data among all 12 populations yielded significant F_{ST} values after a FDR correction (Benjamini and Hochberg 1995) (Table 3). However, all pairwise comparisons of populations within Sleeping Bear Dunes (GHB, SBP, DC, DP, EB, PB, SB) and nearby ZP displayed relatively lower pairwise F_{ST} values (Table 3), suggesting that there is some gene flow among these populations. The AMOVA based on the nSSR data also found that a significant amount of the genetic variation could be explained by differences between populations in the northern region (GM, PS, TC) and populations in the southern region (GHB,

303 SBP, DC, DP, EB, PB, SB, ZP, AD) (F_{CT} = 0.144, $P < 0.0001$), as well as among populations
304 within regions (F_{SC} = 0.097, $P < 0.0001$). However, the majority of the genetic variance was
305 explained by among population differences (F_{ST} = 0.228, $P < 0.0001$).
306 The Bayesian clustering analysis from the program STRUCTURE (Pritchard et al. 2000)
307 partitioned the population into two clusters ($K = 2$) (Figure 2), inferred from both Ln Pr(X|K) and
308 Evanno's ΔK (Supplemental B). This analysis was run without inferring any prior information on
309 sampling location, and then again with sampling information as prior. No differences were
310 observed between the two results (without priors shown in Figure 2). Cluster 1 is comprised of
311 the northernmost populations (GM, PS, TC), and cluster 2 includes all other populations.
312 However, five individuals in the GM population (cluster 1) were assigned to cluster 2
313 (assignment probability > 90%), and these individuals were located at a separate sampling
314 location from the rest in GM. In addition, though there is little admixture overall, several
315 individuals in the GM, TC, EB, and AD populations showed a higher proportion of admixture
316 among the two clusters.
317 The Principal Coordinates analysis (PCoA) based on an individual pairwise genotypic
318 distance matrix highlighted population substructuring (Supplemental C). Individuals in the AD
319 population expanded along both principal coordinates away from individuals assigned to the
320 original STRUCTURE cluster 2 (Figure 2). In addition, the scatterplot supported the strong
321 grouping of individuals in GM, PS, and TC together.
322 A Discriminant Analysis of Principal Components (DAPC) scatterplot (Figure 3a)
323 grouped individuals into three clusters along two axes, supporting the substructuring illustrated
324 in the PCoA. While the PCoA illustrated global diversity found in the nSSR dataset, the DAPC
325 optimizes between group variance. Figure 3b shows the overlap between the distributions of

326 individuals in DAPC clusters 2 and 3 along the first discriminant function, suggesting little
327 distance between them. The membership of individuals of each population to the three illustrated
328 clusters can be seen in Figure 3c. This visualization of the data further highlights the more subtle
329 structure of baby's breath populations in the dunes system of Michigan.

330 A Mantel test for isolation by distance (IBD) performed over all populations found a
331 significant correlation between genetic and geographic distances ($R = 0.755$, $P < 0.001$) (Figure
332 4a). Upon further exploration of this correlation through separate Mantel tests within each
333 identified STRUCTURE cluster, we found a significant correlation within cluster 2 (Figure 4c)
334 ($R = 0.523$, $P = 0.030$), but no significant correlation within cluster 1 (Figure 4b) ($R = 0.205$, $P =$
335 0.494).

336 The AMOVA based on $\mathbf{\Phi}_{ST}$ distance (Supplemental D) facilitated the comparison
337 between the nSSR and cpSSR data, which resulted in a significant amount of the genetic
338 variation explained by differences among regions (nSSR $\mathbf{\Phi}_{CT} = 0.226$, cpSSR $\mathbf{\Phi}_{CT} = 0.263$),
339 among populations within regions (nSSR $\mathbf{\Phi}_{SC} = 0.167$, cpSSR $\mathbf{\Phi}_{SC} = 0.643$), and within
340 populations (nSSR $\mathbf{\Phi}_{ST} = 0.355$, cpSSR $\mathbf{\Phi}_{ST} = 0.736$) for both data sets ($P < 0.0001$).

341 For the cpSSR markers, the minimum spanning network illustrates the distribution of
342 haplotypes across the 12 populations (Figure 5). Five haplotypes were found; Haplotype 1 was
343 the most common, but only occurred in the SBDNL and ZP populations (GHB, SBP, DC, DP,
344 EB, PB, SB, ZP). Haplotype 2 was private to the SB and ZP populations, but rare, occurring in
345 one and two individuals, respective to the populations. Haplotype 3 was private to the five GM
346 individuals located separately from the majority of the other individuals from the GM
347 population. Haplotype 4 was private to SB, ZP, and AD populations, and occurred in all AD

348 individuals, but was less common in the SB and ZP populations. Haplotype 5 was private to GM,
349 PS, and TC populations, occurring in all individuals.
350
351 **DISCUSSION**
352 The natural disturbance regime of dynamic sand dune systems can result in a pattern of
353 fragmented habitat and often sparse vegetative cover, making dune ecosystems highly
354 susceptible to plant invasions (Jorgensen and Kollman 2009, Carranza et al. 2010, Rand et al.
355 2015). The topography, geographic distribution of preferred habitat, and disturbance regime in
356 an ecosystem can influence various stages of a species invasion, including where the plant
357 establishes, its dispersal patterns, and how densely it grows (With 2002, Theoharides and Dukes
358 2007). In addition, the demographic processes of an introduction event can shape contemporary
359 population dynamics (Dlugosch and Parker 2008, Estoup and Guillemaud 2010). The invasion of
360 baby's breath in the Michigan dune system is an opportunity to better understand the genetic
361 structure of invasive species in this system and how the dynamic landscape of these dunes may
362 be shaping it. Our results indicate variation in genetic diversity among populations, as well as
363 strong genetic structure that clusters individuals into two distinct groups. These two groups are
364 separated by a peninsula that could be limiting gene flow between the two groups, causing this
365 genetic separation.
366 We observed moderate levels of nuclear and chloroplast genetic diversity across
367 populations of baby's breath throughout the dune system of Michigan (Table 1). However,
368 genetic diversity in our northern-most populations (Grand Marais, Petoskey State Park, and
369 Traverse City) was typically lower compared to that found in the populations in Sleeping Bear
370 Dunes, Zetterberg Preserve, and Arcadia Dunes. Differences in the level of genetic diversity

among these regions could be due to differences in population size. Sleeping Bear Dunes is a largescale infestation and has some of the highest densities of baby's breath found within the Michigan coastal dunes (TNC 2013), consisting of up to 80% of the vegetation and covering hundreds of acres in some areas. The Grand Marais, Petoskey State Park, and Traverse City populations are much smaller than those found in Sleeping Bear Dunes, with continuous populations often limited to less than 45 acres (TNC 2012 internal report). These smaller populations could be more affected by the impact of genetic drift and potential inbreeding, resulting in the observed lower levels of genetic diversity (Ellstrand and Elam 1993, Young et al. 1996, Keller and Waller 2002).

The level of isolation between Grand Marais, Petoskey State Park, and Traverse City could also be contributing to the lower levels of genetic diversity observed in these areas compared to other populations. F_{ST} values among these three populations ranged from 0.121 – 0.221, which is much higher than the F_{ST} range observed between the Sleeping Bear Dunes, Zetterberg Preserve, and Arcadia Dunes populations (0.041 – 0.137). This suggests that our northern-most populations may have less gene flow between neighboring populations. This could be the result of larger geographic distances between these locations. For example, Grand Marais is located in Michigan's upper peninsula while Petoskey State Park and Traverse City are located in the lower peninsula. Higher levels of isolation could also be a result of decreased availability of suitable habitat, which may be more limited between these areas. Sleeping Bear Dunes and nearby surrounding areas make up a large contiguous amount of land that has been preserved by the National Parks Service, The Nature Conservancy, and other local land conservancies. Thus, the dune habitat is often continuous, with limited human development. On the other hand, Traverse City, Petoskey State Park, and Grand Marais areas have more human development

394 along the lakeshore, which may provide additional barriers to gene flow among these
395 populations.

396 Management histories could also be contributing to the differences in genetic diversity
397 seen among these populations of baby's breath. The entire Petoskey State Park population was
398 treated with herbicide or manual removal from 2007 – 2012 by The Nature Conservancy. At this
399 time, managers considered the population to be at a desirable management level, and it has been
400 unmanaged since (TNC 2012 internal report). It is possible that the intensive management
401 resulted in a population bottleneck, and the population rebound following 2012 came from a
402 reduced number of individuals leading to the reduced genetic diversity that we observe today.
403 However, this is probably not the only reason for the lower levels observed. The Arcadia Dunes
404 and Zetterberg Preserve populations have also been regularly managed since 2004 and 2007,
405 respectively, so if management is solely driving these patterns we would expect Arcadia Dunes
406 and Zetterberg Preserve to also have reduced genetic diversity. Although the Arcadia Dunes
407 population does have the lowest allelic richness and heterozygosity of all the populations in
408 cluster 2 (Figure 2), both populations have relatively high genetic diversity despite over ten years
409 of management. It is possible that higher levels of gene flow between these populations and
410 those in Sleeping Bear Dunes may be helping to maintain genetic diversity. F_{ST} values between
411 Zetterberg Preserve and other populations in Sleeping Bear Dunes range from 0.017 – 0.090,
412 suggesting some gene flow, particularly with the population at the southern boundary (SB) of
413 Sleeping Bear Dunes. Furthermore, infestations on private properties adjacent to Zetterberg
414 Preserve have presumably buffered the population sizes. Given Petoskey State Park's geographic
415 distance from Sleeping Bear Dunes, limited gene flow between them would prevent the
416 maintenance of high genetic diversity after intense management.

417 The topography and habitat heterogeneity of the dune system likely contributes to the
418 pattern of population structure of baby's breath throughout the Michigan dunes. Habitat
419 heterogeneity can drive population structure, with variation in habitat type within the dunes
420 acting as barriers to dispersal (Henry et al. 2009, Fant et al. 2014). Baby's breath is typically
421 found in open back dune habitat, but has also been found in the fore dunes close to the lake
422 beach and on steep dune sides. However, forested areas that are part of the back dunes have been
423 identified by land managers as barriers between populations, preventing population spread of
424 baby's breath (personal communication, Shaun Howard and Jon Throop). This can lead to
425 populations in relatively close proximity to one another showing high levels of genetic
426 differentiation and is likely a contributor to the significant population structure found among the
427 populations in Sleeping Bear Dunes. For example, the Empire Bluff population (EB) is located
428 on the tip of a dune bluff: a small visitor outlook point surrounded by forest, and seems to be
429 isolated from nearby populations. Despite its geographic proximity to Platte Bay (PB) (8.22 km),
430 it is more genetically similar to Sleeping Bear Point (SBP), a population 12.73 km away (F_{ST} =
431 0.106 and F_{ST} = 0.069 respectively).
432 A Mantel test for isolation by distance (IBD) revealed a moderate positive relationship
433 between nSSR genetic distances (based on transformed pairwise F_{ST} values) and geographic
434 distances (straight-line distances in km) of all populations (Figure 4a), and was also found for the
435 analysis of populations in STRUCTURE cluster 2 (Figure 4c). However, when examining the
436 IBD relationship within cluster 1 from the STRUCTURE analysis, this positive relationship is
437 not significant (Figure 4b). We attribute the overall significant relationships found (Figure 4a and
438 4c) to the strong genetic differences between populations in the two main clusters, as well as the
439 genetic difference of the Arcadia Dunes population when compared to Zetterberg Preserve and

Sleeping Bear Dunes populations. Though geographic distance possibly influences the strong structuring of distant populations, the isolating effect of the topography within the dunes could have an effect that overrides that of geographic distance, particularly on smaller spatial scales such as that observed in Sleeping Bear Dunes. These results further support the strong regional differences between the two clusters identified in the Bayesian analysis (Figure 2).

The tumbleweed mechanism of dispersal that baby's breath employs could be an effective means to disperse seeds, but it is possible that the strong topographical structure, habitat heterogeneity and variable weather patterns within the dunes impact seed dispersal for gene flow more than they impact pollination. Baby's breath has been found to attract a diverse array of pollinator species (Baskett et al. 2011, Emery and Doran 2013), sometimes at the expense of native plant pollination, while seed dispersal is primarily limited to wind-driven tumbleweeds. The variation in $\mathbf{\Phi}_{ST}$ values between the two marker types (nSSR $\mathbf{\Phi}_{ST} = 0.355$, cpSSR $\mathbf{\Phi}_{ST} = 0.736$) indicates that barriers to seed dispersal may be more limiting for gene flow than pollination. Darwent (1975) also suggested that though seeds could be dispersed up to 1 km, many of the seeds were released near the parent plant prior to the stems tumbling. This could result in strong population structure due to a lower frequency of migrants. Therefore, the elements of the dune ecosystem could be impacting gene flow through seed dispersal by further limiting the plant's ability to spread throughout the landscape. However, these comparison of cpSSR results to nSSR should be taken with some caution, as we had a limited number of polymorphic cpSSR markers. Though we chose to use microsatellites within the chloroplast genome to increase the likelihood of polymorphism, we still found these regions to be well-conserved and with limited variation in our dataset. Therefore, we cannot rule out the

462 possibility of fragment size homoplasy confounding results of low genetic diversity in some
463 populations (Bang and Chung 2015).
464
465 **Structure analysis**
466 Our results from the Bayesian clustering analysis in STRUCTURE (Pritchard et al. 2000,
467 Evanno et al. 2005) separate the populations of baby's breath along the Michigan coastal dunes
468 into two genetic clusters ($K = 2$) (Figure 2). A similar pattern was found when the nSSR dataset
469 was analyzed using a PCoA (Supplemental C) and a DAPC (Figure 3), with the exception that
470 the individuals of the Arcadia Dunes population further separated from the Sleeping Bear Dunes
471 and Zetterberg Preserve individuals in the latter analyses. The clusters are mainly divided into
472 the Traverse City, Petoskey State Park, and Grand Marais cluster (cluster 1) and the Sleeping
473 Bear Dunes populations, Zetterberg Preserve, and Arcadia Dunes cluster (cluster 2). The
474 distribution of cpSSR haplotypes (Figure 5) across populations further illustrates the strong
475 genetic clusters present in this dataset. Specifically, some haplotypes are only found in certain
476 populations and within each main population cluster. Haplotypes 1, 2, and 4 only occur in
477 populations in cluster 2. Haplotypes 3 and 5 only occur in cluster 1, with haplotype 3 being
478 private to the five individuals in Grand Marais that were located separately from the rest of those
479 sampled at this location (Figure 5). The two distinct population clusters are separated by the
480 Leelanau peninsula, which may be helping to limit gene flow among these clusters. This
481 partitioning of cpSSR haplotypes could be due to seed dispersal limitations from habitat
482 fragmentation, unsuitable habitat, and land use, as the peninsula is comprised mainly of private
483 residential properties along the narrow shoreline.

Understanding the invasion history of a species can help shed light on the factors and processes that contributed to the success of the species establishment. For baby's breath, it has been assumed that invasive populations were the result of ornamental plants escaping from gardens or being purposely planted for horticultural means (personal communication with TNC managers). Whether the clusters we observed for our dataset are the result of multiple independent introductions or the result of one introduction followed by serial invasions is not known. Given that populations along coastal Michigan cluster into two distinct groups, either scenario is possible (Lombaert et al. 2018). In the serial invasion scenario, a founder population would have colonized one site in the Michigan coastal dunes, and then migrants from that population would have invaded subsequent areas (Lombaert et al. 2018). Over time, with limited gene flow, these populations could have become distinct and structured. However, we think this scenario may not be the best explanation for this invasion. Based upon herbarium records, the first occurrence of baby's breath in northwest Michigan was recorded in 1913 in Emmet County where Petoskey State Park is located (Emmet Co., 1913, catalog: 355638, *Gleason s.n.*, MICH). Records from Leelanau and Benzie counties, where Sleeping Bear Dunes, Zetterberg Preserve and Arcadia Dunes are located, were not collected until the late 1940's (Leelanau Co., 1947, catalog: 355348, *P.W. Thompson L-302,* MICH). If Petoskey State Park was the founding population for this invasion, we would expect higher genetic diversity in this population relative to those in Sleeping Bear Dunes, Zetterberg Preserve, and Arcadia Dunes, since a serial introduction would result in additional bottlenecks from the founding population. However, we observed the opposite pattern of genetic diversity. Additionally, there are private cpSSR haplotypes to each of these two clusters (Figure 5), a pattern we would not expect to see if all the populations came from one introduction event.

507 The other invasion scenario describes at least two independent introductions to the
508 Michigan coastal dunes (Lombaert et al. 2018). In this scenario, we would expect strong genetic
509 differentiation between the two or more founding populations. Our data supports this, as we
510 observed both nSSR and cpSSR alleles privately shared only between populations within the
511 same cluster. In addition, for the cpSSR markers, distinct haplotypes were found between the
512 two regions, with haplotype 5 only observed in the Grand Marais, Petoskey State Park, and
513 Traverse City cluster while haplotypes 1, 2, and 4 were only found in the Sleeping Bear Dunes,
514 Zetterberg Preserve, and Arcadia Dunes cluster. There was also a high proportion of nSSR
515 alleles common to both clusters, but this could be the result of limited genetic diversity in the
516 initial source populations (Allendorf and Lundquist 2003). This scenario is particularly plausible,
517 as the source populations would likely be a type of horticultural strain, given the popularity of
518 perennial baby's breath in the floral industry (Vettori et al. 2013, Calistri et al. 2014). This
519 hypothesis of at least two independent introductions also agrees with the herbarium record: a
520 potential introduction event could have occurred in the early 1910's, leading to cluster 1 (GM,
521 PS, TC), and a separate introduction event could have occurred in the late 1940's, leading to the
522 establishment of the populations in Zetterberg Preserve and Sleeping Bear Dunes (cluster 2).
523 In addition to supporting the identified patterns in the nSSR dataset produced from the
524 STRUCTURE analysis, the PCoA and DAPC (Supplemental C and Figure 3) allowed us to
525 identify more subtle population structuring. Specifically, the PCoA (Supplemental C) illustrates
526 the Arcadia Dunes population separating from the other populations along principal coordinate 2.
527 The DAPC (Figure 3) also shows the subtler variation among populations within the Sleeping
528 Bear Dunes populations (specifically Figure 3c), and continues to support the segregation of the
529 Grand Marais, Petoskey State Park, and Traverse City populations from the rest that we see in

530 the STRUCTURE analysis (Figure 2). Variation in allele frequencies and decreased allelic
531 richness are two factors that could explain the divergence of the Arcadia Dunes population in the
532 PCoA (Supplemental C); there are no private alleles or other obvious patterns causing this
533 population to cluster separately from nearby populations (Zetterberg Preserve and South
534 Boundary in Sleeping Bear Dunes). The higher rates of admixture between the two main clusters
535 in Arcadia Dunes individuals (Figure 2) could also be a reason for its slight divergence from
536 cluster 2. However, what is driving this potential higher level of admixture in the Arcadia Dunes
537 population compared to others is currently unknown. Arcadia Dunes is a popular recreation area
538 among locals and tourists (personal communication Jon Throop, Grand Traverse Regional Land
539 Conservancy). Additionally, the autumn season brings about a high volume of foot traffic
540 through all the dune areas of Michigan. It is possible that people may be accidentally
541 transporting baby's breath seeds between these otherwise isolated populations, as the seed
542 phenology coincides with the autumn senescence. While human transport of seeds may be
543 occurring at other locations as well, Arcadia Dunes is a small enough population that newly
544 introduced genotypes could have a higher likelihood of being detected from sampling relative to
545 other larger populations, such as one in Sleeping Bear Dunes.
546 The invasion of baby's breath to the Great Lakes has the potential to disrupt the
547 dynamism of the dune landscape and biological community in northwest Michigan, and this
548 threat has led to increased concern over its pervasiveness regionally and nationally. Estimating
549 the genetic structure of invasive populations can lead to a better understanding of the invasion
550 history and the factors influencing the success of an invasion (Crosby et al. 2014, Piya et al.
551 2014, Sakata et al. 2015). Through population level analysis, we found strong genetic structure
552 present that separates the invasion in the Michigan dunes into two main regions. Based on these

553 results, we suggest that the contemporary baby's breath population within the Michigan coastal
554 dune system is the result of at least two separate introduction events. The genetic structure
555 identified for these baby's breath populations probably results from a combination of
556 demographic processes –multiple introductions, bottleneck events, isolation, and admixture,
557 along with landscape level processes. The topography of the dunes is heterogeneous but also
558 constantly shifting, and the baby's breath invasion is one example of how this dynamic system
559 can shape the establishment, gene flow, and spread of invasive plant populations.
560
561
562
563
564
565
566
567
568
569
570
571
572
573
574
575

ACKNOWLEDGEMENTS

The authors thank the Environmental Protection Agency – Great Lakes Restoration Initiative Grant (C.G.P., Grant #00E01934) for financial support. We thank Dr. James McNair for assistance with statistical analyses, Dr. Timothy Evans for assistance with herbarium data expertise and submission, and Kurt Thompson for assistance with geographic data collection and visualization. Finally, we thank Emma Rice for all her assistance in field data collection and Matthew Kienitz for his assistance in field and laboratory data collection.

CONFLICT OF INTEREST

The authors declare there is no conflicts of interest associated with this study.

DATA ARCHIVING

All genotype data will be submitted to the Dryad Digital Repository upon acceptance. Nuclear microsatellite sequences have been deposited to GenBank (Table 1).

599 **REFERENCES**

600 Albert DA (2000). *Borne of the Wind, Michigan Sand Dunes*. University of Michigan Press:
601 Michigan.
602
603 Allendorf FW, Lundquist LL (2003). Introduction: population biology, evolution, and control of
604 invasive species. *Conserv Biol* **17**: 24 – 30.
605
606 Arbogast AF (Department of Geography, Michigan State University, Lansing, MI). The
607 Emerging Science of Coastal Sand Dune Age and Dynamics: Implications for Regulation and
608 Risk Management in Michigan. Lansing, MI: *Michigan Environmental Council*: May 2015. 45 p.
609 Website
610 https://d3n8a8pro7vhmx.cloudfront.net/environmentalcouncil/pages/467/attachments/original/15
611 18314397/Latest_Science-Michigan_Coastal_Dunes.pdf?1518314397%22 [accessed 06 October
612 2017].
613
614 Arbogast AF, Loope WL (1999). Maximum-limiting ages of Lake Michigan coastal dunes: Their
615 correlation with Holocene lake level history. *J Great Lakes Res* **25**: 372-382.
616
617 Archer FI, Adams PE, Schneiders BB (2016). STRATAG: An R package for manipulating,
618 summarizing and analysing population genetic data. *Mol Ecol Resour* **17**: 5–11.
619
620 Baker HG (1986). Patterns of plant invasion in North America. In: Mooney HA, Drake JA (eds)
621 *Ecology of Biological Invasions of North America and Hawaii*. Springer, New York, pp 44–57.
622
623 Bang SW, Chung S-M (2015). One size does not fit all: the risk of using amplicon size of
624 chloroplast SSR marker for genetic relationship studies. *Plant Cell Rep* **34**: 1681 – 1683.
625
626 Baskett CA, Emery SM, Rudgers JA (2011). Pollinator Visits to Threatened Species Are
627 Restored Following Invasive Plant Removal. *Int J Plant Sci* **172**: 411–422.
628
629 Benjamini Y, Hochberg Y (1995). Controlling The False Discovery Rate - A Practical And
630 Powerful Approach To Multiple Testing. *J R Stat Soc Series B Stat Methodol* **57**: 289 - 300.
631
632 Blumer BE, Arbogast AF, Forman SL (2012). The OSL chronology of eolian sand deposition in
633 a perched dune field along the northwestern shore of Lower Michigan. *Quat Int* **77**: 445 – 455.
634
635 Bustamante RO, Durán AP, Peña-Gómez FT, Véliz D (2018). Genetic and phenotypic variation,
636 dispersal limitation and reproductive success in the invasive herb *Eschscholzia californica* along
637 an elevation gradient in central Chile. *Plant Ecol Divers* **10**: 419 – 429.
638

639 Calistri E, Buiatti M, Bogani P (2014). Characterization of *Gypsophila* species and commercial
640 hybrids with nuclear whole-genome and cytoplasmic molecular markers. *Plant Biosyst* **150**: 11 –
641 21.
642
643 Carranza ML, Carboni M, Feola S, Acosta ATR (2010). Landscape-scale patterns of alien
644 species on coastal dunes: the case of iceplant in central Italy. *Appl Veg Sci* **13**: 135-145.
645
646 Chung S-M, and Staub JE (2003). The development and evaluation of consensus chloroplast
647 primer pairs that possess highly variable sequence regions in a diverse array of plant taxa. *Theor*
648 *Appl Genet* **107**: 757–767.
649
650 Cowles HC (1899). The Ecological Relations of the Vegetation on the Sand Dunes of Lake
651 Michigan. Part I.-Geographical Relations of the Dune Floras. *Bot Gaz* **27**: 95 – 117.
652
653 Crosby K, Stokes TO, Latta RG (2014). Evolving California genotypes of *Avena barbata* are
654 derived from multiple introductions but still maintain substantial population structure. *PeerJ* **2**:
655 e633.
656
657 Cusseddu V, Ceccherelli G, Bertness M (2016). Hierarchical organization of a Sardinian sand
658 dune plant community. *PeerJ* **4**: e2199.
659
660 Darwent AL (1975). The Biology of Canadian Weeds. 14. *Gypsophila paniculata* L. *Canadian*
661 *Journal of Plant Science* **55**: 1049–1058.
662
663 Darwent AL, Coupland RT (1966). Life history of *Gypsophila paniculata*. *Weeds* **14**: 313–318.
664
665 Dewoody J, Nason JD, Hipkins VD (2006). Mitigating scoring errors in microsatellite data from
666 wild populations. *Mol Ecol Notes* **6**: 951–957.
667
668 Dlugosch KM, Parker IM (2008). Founding events in species invasions: Genetic variation,
669 adaptive evolution, and the role of multiple introductions. *Mol Ecol* **17**: 431 – 449.
670
671 Department of Natural Resources (DNR) (2015). Michigan Invasive Species Grant Program
672 Handbook. Website http://www.michigan.gov/documents/dnr/2015-MISGP-
673 hndbk_491809_7.pdf?source=govdelivery [accessed 05 March 2018].
674
675 Eliades N-G, Eliades DG (2009). HAPLOTYPE ANALYSIS: Software for analysis of haplotype
676 data. (available from http://www.uni-goettingen.de/en/134935.html)
677

678 Ellstrand NC, Elam DR (1993). Population Genetic Consequences of Small Population Size:
679 Implications for Plant Conservation. *Annu Rev Ecol Syst* **24**: 217-242.
680
681 Emery SM, Doran PJ (2013). Presence and management of the invasive plant *Gypsophila*
682 *paniculata* (baby's breath) on sand dunes alters arthropod abundance and community structure.
683 *Biol Cons* **161**: 174–181.
684
685 Estoup A, Guillemaud T (2010). Reconstructing routes of invasion using genetic data: why, how
686 and so what. *Mol Ecol* **19**: 4113 – 4130.
687
688 Evanno G, Regnaut S, Goudet J (2005). Detecting the number of clusters of individuals using the
689 software STRUCTURE: A simulation study. *Mol Ecol* **14**: 2611–2620.
690
691 Everard M, Jones L, Watts B (2010). Have we neglected the societal importance of sand dunes?
692 An ecosystem services perspective. *Aquat Conserv* **20:** 476–487.
693
694 Excoffier L, Smouse PE, Quattro JM (1992). Analysis of molecular variance inferred from
695 metric distances among DNA haplotypes: application to human mitochondrial DNA restriction
696 sites. *Genetics* **131**: 479 – 491.
697
698 Fant JB, Havens K, Keller JM, Radosavljevic A, Yates ED (2014). The influence of
699 contemporary and historic landscape features on the genetic structure of the sand dune endemic,
700 *Cirsium pitcheri* (Asteraceae). *Heredity* **112**: 519 – 530.
701
702 Gomes I, Collins A, Lonjou C, Thomas NS, Wilkinson J, Watson M *et al.* (1999). Hardy–
703 Weinberg quality control. *Ann Hum Genet* **63**: 535–538.
704
705 Grime, J. P. 1979. *Plant Strategies and Vegetation Processes*. John Wiley and Sons: Chichester,
706 UK.
707
708 Guichoux E, Lagache L, Wagner S, Chaumeil P, Léger P, Lepais O *et al.* (2011). Current trends
709 in microsatellite genotyping. *Mol Ecol Resour* **11**: 591–611.
710
711 Hagenblad J, Hülskötter J, Acharya KP, Brunet J, Chabrerie O, Cousins SA *et al* (2015). Low
712 genetic diversity despite multiple introductions of the invasive plant species *Impatiens*
713 *glandulifera* in Europe. *BMC Genet* **16**:103.
714
715 Henry P, Le Lay G, Goudet J, Guisan A, Jahodová S, Besnard G (2009). Reduced genetic
716 diversity, increased isolation and multiple introductions of invasive giant hogweed in the western
717 Swiss Alps. *Mol Ecol* **18**: 2819–2831.

Jolls CL, Marik JE, Hamzé SI, Havens K (2015). Population viability analysis and the effects of light availability and litter on populations of *Cirsium pitcheri*, a rare, monocarpic perennial of Great Lakes shorelines. *Biol Cons* **187**: 82–90.

Jombart T (2008). adegenet: a R package for the multivariate analysis of genetic markers. *Bioinformatics* **24**: 1403 – 1405.

Jombart T, Devillard S, Balloux F (2010). Discriminant analysis of principal components: A new method for the analysis of genetically structured populations. *BMC Genet* **11**: 94.

Jorgensen RH, Kollman J (2009). Invasion of coastal dunes by the alien shrub *Rosa rugosa* is associated with roads, tracks and houses. *Flora – Morphology, Distribution, Functional Ecology of Plants* **204**: 289-297.

Kamvar ZN, Tabima JF, Grünwald NJ (2014). Poppr: An R Package For Genetic Analysis Of Populations With Clonal, Partially Clonal, And/or Sexual Reproduction. *PeerJ* **2**: e281.

Keenan K, McGinnity P, Cross TF, Crozier WW, Prodöhl PA, O'Hara RB (2013). diveRsity: An R package for the estimation and exploration of population genetics parameters and their associated errors. *Methods Ecol Evol* **4**: 782 – 788.

Keller LF, Waller DM (2002). Inbreeding effects in wild populations. *Trends Ecol Evol* **17**: 230 – 241.

Kopelman NM, Mayzel J, Jakobsson M, Rosenberg NA, Mayrose I (2015). CLUMPAK: a program for identifying clustering modes and packaging population structure inferences across K. *Mol Ecol Resour* **15**: 1179 – 1191.

Leimbach-Maus H, Parks S, Partridge C (2018). Microsatellite primer development for invasive perennial herb, *Gypsophila paniculata* (Caryophyllaceae). *bioRxiv* https://doi.org/10.1101/401398.

Lombaert E, Guillemaud T, Deleury E (2018). Biases of STRUCTURE software when exploring introduction routes of invasive species. *Heredity* **120**: 485 – 499.

Michigan, Emmet Co.: Pellston, 16 July 1913, *H.A. Gleason s.n.* (MICH).

Michigan, Leelanau Co.: Leland Twp, 05 August 1947, *P.W. Thompson L-302* (MICH).

Moran EV, Reid A, Levine JM (2017). Population genetics and adaptation to climate along elevation gradients in invasive *Solidago canadensis*. *PLoS ONE* **12**: e0185539.

Nagy AM, Korpelainen H (2014). Population genetics of Himalayan balsam (*Impatiens glandulifera*): comparison of native and introduced populations. *Plant Ecol Divers* **8**: 317 – 321.

Olson JS (1958). Rates of Succession and Soil Changes on Southern Lake Michigan Sand Dunes. *Bot Gaz* **119**: 125 – 170.

Peakall R, Smouse PE (2006). GENALEX 6: genetic analysis in Excel. Population genetic software for teaching and research. *Mol Ecol Notes* **6**: 288 – 295.

Peakall R, Smouse PE (2012). GenAlEx 6.5: genetic analysis in Excel. Population genetic software for teaching and research-an update. *Bioinformatics* **28**: 2537 – 2539.

Peakall R, Smouse PE, Huff DR (1995). Evolutionary implications of allozyme and RAPD variation in diploid populations of dioecious buffalograss *Buchloe dactyloides. Mol Ecol* **4**: 135-147.

Piya S, Nepal MP, Butler JL, Larson GE, Neupane A (2014). Genetic diversity and population structure of sickleweed (*Falcaria vulgaris*; Apiaceae) in the upper Midwest USA. *Biol Invasions* **16**: 2115–2125.

Pritchard JK, Stephens M, Donnelly P (2000). Inference of population structure using multilocus genotype data. *Genetics* **155**: 945–959.

Raymond M, Rousset F (1995). GENEPOP (version 4.2): Population genetics software for exact tests and ecumenicism. *J Hered* **86**: 248–249.

Rand TA, Louda SM, Bradley KM, Crider KK (2015). Effects of invasive knapweed (*Centaurea stoebe* subsp. micranthos) on a threatened native thistle (*Cirsium pitcheri*) vary with environment and life stage. *Botany* **93**: 543–558.

Rousset F (2008). Genepop'007: a complete reimplementation of the Genepop software for Windows and Linux. *Mol Ecol Resour* **8**: 103 – 106.

Sakai AK, Allendorf FW, Holt JS, Lodge DM, Molofsky J, With KA et al (2001). The population biology of invasive species. *Annu Rev Ecol Syst* **32**: 305–332.

797 Sakata Y, Itami J, Isagi Y, Ohgushi T (2015). Multiple and mass introductions from limited
798 origins: genetic diversity and structure of *Solidago altissima* in the native and invaded range. *J*
799 *Plant Res* **128:** 909–921.
800
801 Slatkin M (1995). A measure of population subdivision based on microsatellite allele
802 frequencies. *Genetics* **139**: 457 – 462.
803
804 Smouse PE, Long JC, Sokal RR (1986). Multiple regression and correlation extensions of the
805 mantel test of matrix correspondence. *Syst Biol* **35**: 627 – 632.
806
807 Smouse PE, Long JC (1992). Matrix correlation analysis in anthropology and genetics. *Am J*
808 *Phys Anthropol* **35**: 187 – 213.
809
810 Smouse PE, Peakall R (1999). Spatial autocorrelation analysis of individual multiallele and
811 multilocus genetic structure. *Heredity* **82**: 561 – 573.
812
813 The Nature Conservancy and partners. (2013). Lake Michigan Coastal Dunes Restoration
814 Report. The Nature Conservancy. Website
815 https://www.nature.org/ourinitiatives/regions/northamerica/unitedstates/michigan/lake-michigan-
816 dune-report-2013.pdf [accessed 01 November 2017].
817
818 Theoharides KA, Dukes JS (2007). Plant invasion across space and time: factors affecting
819 nonindigenous species success during four stages of invasion. *New Phytol* **176:** 256 – 273.
820
821 Van Oosterhout C, Hutchinson WF, Wills DPM, Shipley P (2004). MICRO-CHECKER:
822 software for identifying and correcting genotyping errors in microsatellite data. *Mol Ecol Resour*
823 **4**: 535–538.
824
825 Van Oosterhout C, Weetman D, Hutchinson WF (2006). Estimation and adjustment of
826 microsatellite null alleles in nonequilibrium populations. *Mol Ecol Resour* **6**: 255–256.
827
828 Vettori L, Schiff S, Tani C, Pasqualetto P, Bennici A (2013). Morphological and cytological
829 observations of wild species and hybrids of *Gypsophila*. *Plant Biosyst* **150**: 1 – 11.
830
831 Weir B, Cockerham C (1984). Estimating F-Statistics for the Analysis of Population
832 Structure. *Evolution* **38**: 1358 – 1370.
833
834 With KA (2002). The landscape ecology of invasive spread. *Conserv Biol* **16**: 1192 – 1203.
835

836 Xu C-Y, Tang S, Fatemi M, Gross CL, Julien MH, Curtis C *et al.* (2015). Population structure
837 and genetic diversity of invasive *Phyla canescens*: implications for the evolutionary potential.
838 *Ecosphere* **6**: 162.
839
840 Young A, Boyle T, Brown T (1996). The population genetic consequences of habitat
841 fragmentation for plants. *Trends Ecol Evol* **11**: 413 – 418.
842
843 Zarnetske PL, Seabloom EW, Hacker SD (2010). Non-target effects of invasive species
844 management: beachgrass, birds, and bulldozers in coastal dunes. *Ecosphere* **1**: art13.
845

846

847

848

849

850
851
852
853
854
855
856
857
858
859
860
861
862
863
864
865
866
867
868
869
870
871
872
873
874
875

FIGURE LEGENDS

Figure 1 Map of baby's breath sampling locations in Michigan. Seven were located throughout Sleeping Bear Dunes National Lakeshore. Park boundary delineated by grey shading in bottom left panel. Sampling location codes: Grand Marais (GM), Petoskey State Park (PS), Traverse City (TC), Good Harbor Bay (GHB), Sleeping Bear Point (SBP), Dune Climb (DC), Dune Plateau (DP), Empire Bluffs (EB), Platte Bay (PB), South Boundary (SB), Zetterberg Preserve (ZP), Arcadia Dunes (AD).

Figure 2 Results from Bayesian cluster analysis based on nSSR data using the program STRUCTURE (Pritchard et al. 2000) indicate ($K = 2$) population clusters of baby's breath (Pritchard et al. 2000, Evanno et al. 2005). Cluster 1 (left) includes the three northernmost populations, and Cluster 2 (right) includes all other populations. Each individual ($N = 313$) is represented by a line in the plot, and individuals are grouped by population.
Sampling location codes: Grand Marais (GM), Petoskey State Park (PS), Traverse City (TC), Good Harbor Bay (GHB), Sleeping Bear Point (SBP), Dune Climb (DC), Dune Plateau (DP), Empire Bluffs (EB), Platte Bay (PB), South Boundary (SB), Zetterberg Preserve (ZP), Arcadia Dunes (AD).

Figure 3 Discriminant analysis of principal components (DAPC) based on baby's breath nSSR data and calculated in the *adegenet* v2.1.0 (Jombart 2008, Jombart et al. 2010) package for R. (A) Scatterplot of both discriminant function axes; all individuals ($n = 313$) are included and represented by a dot. (B) Plot of DAPC sample distribution on discriminant function 1. (C) Table of individual membership to each DAPC cluster, explained by the PCA eigenvalues used in the DAPC, based on all 69 identified principal components.
Sampling location codes: Grand Marais (GM), Petoskey State Park (PS), Traverse City (TC), Good Harbor Bay (GHB), Sleeping Bear Point (SBP), Dune Climb (DC), Dune Plateau (DP), Empire Bluffs (EB), Platte Bay (PB), South Boundary (SB), Zetterberg Preserve (ZP), Arcadia Dunes (AD).

Figure 4 Mantel tests using transformed pairwise population F_{ST} values of nSSR data (Slatkin 1995) and straight-line distances (km) between populations based on the mean center latitude and longitude of each location. (A) Between all populations, (B) between populations in the Northern region (cluster 1), and (C) between populations in the Southern region (cluster 2) identified from the Bayesian clustering analysis. Reported p-values based on the one-sided alternative hypothesis (H^1: $R > 0$).

Figure 5 Minimum spanning network based on Nei's genetic distance (Nei 1972) matrix of baby's breath cpSSR data. Created in the *poppr* v2.8.0 package (Kamvar et al. 2014) for R. Illustrates the distribution of haplotypes across the 12 populations. Haplotype size indicates frequency in populations.

Sampling location codes: Grand Marais (GM), Petoskey State Park (PS), Traverse City (TC), Good Harbor Bay (GHB), Sleeping Bear Point (SBP), Dune Climb (DC), Dune Plateau (DP), Empire Bluffs (EB), Platte Bay (PB), South Boundary (SB), Zetterberg Preserve (ZP), Arcadia Dunes (AD).

957

Table 1 Characteristics of 14 nSSR loci developed for baby's breath and 2 universal cpSSR loci used in this study.

Locus[a]	Primer sequences (5' - 3')	Repeat motif	Allele size range (bp)	Annealing temperature (℃)	Fluorescent label	Multiplex	GenBank accession no.
nSSR Loci							
BB_21680	F: ACTACACACAGACTCGATCCTC R: CTTTGATTGTTTGGTGTAAGTTGC	$(AAAG)_5$	199 - 218	62	PET	PS1	MH704705
BB_6627	F: CAAACTCAACCAACCAGACACC R: CACCTCAGCAACAACAGAGTG	$(AAAC)_5$	151 - 155	62	FAM	PS1	MH704715
BB_3968	F: CATGGAGGACAATGAGAAGACG R: ACGGTGGTAATGAAGTTTGGTG	$(AGG)_6$	207 - 219	62	FAM	PS2	MH704706
BB_5151	F: TCCACCTTATAACTCACCACCC R: TGAGGAAGGATAACAGCTCTCG	$(ACC)_5$	205 - 210	62	PET	PS2	MH704712
BB_4443	F: TAGGGTGGGTGCTTGTACTAAC R: AAAGTGGTGCTGCAGAAGAATC	$(AAG)_{16}$	171 - 211	62	NED	PS2	MH704704
BB_31555	F: TGTATAACTGAGATAACCCAGACG R: TTGTTACCTTGTTCCGGCAAAG	$(AC)_7$	150 - 156	62	VIC	PS2	MH704716
BB_14751[b]	F: CCTCAAACCCTAACAATGCTCC R: TCAGCCGATCCTCTAACACG	$(AAG)_{12}$	195 - 248	62	FAM	PS3	MH704713
BB_3335[b]	F: TCCACCAAACTCTTAAACTGCC R: CACAGACACAAAGGATCCAACC	$(AGG)_5$	215 - 244	62	NED	PS3	MH704701
BB_4258[b]	F: TCACAAGAGGCCCAATTTCTTC R: ACTTGAACCCGAACCTATACCC	$(AAT)_5$	178 - 195	62	VIC	PS3	MH704714
BB_3913	F: GGCTGTCGGGTAATAAACACAG R: TCCCAACTCAAGTCATAGCCTAG	$(ACAG)_5$	159 - 171	62	PET	PS3	MH704702
BB_2888[b]	F: CTTCATTCATGTACAAGAGCGC R: AGAACTGGCTATGGATCGAAATG	$(AC)_{16}$	219 - 232	63	FAM	PS4	MH704709
BB_5567	F: GGCTAGGGAAAGTAGGAAGACC R: CGTGTCCTGTTTCTCCATGATC	$(AAT)_5$	198 - 222	62	VIC	PS4	MH704703
BB_7213[b]	F: TTGCATTCCCACCATTTCATCC R: AGCCAACCTCGTATTAATTGCC	$(AC)_7$	161 - 248	62	PET	PS4	MH704708
BB_8681[b]	F: ATCTCCAGTTTCCGTGATTTGC R: TACGTCACAAGAGCTTTCAACC	$(ACC)_8$	204 - 222	62	NED	PS5	MH704710
cpSSR Loci							
ccssr4	F: AGGTTCAAATCCTATTGGACGCA R: TTTTGAAAGAAGCTATTCARGAAC	$(T)_8$	204 - 219	52	NED	–	–
ccssr9	F: GAGGATACACGACAGARGGARTTG R: CCTATTACAGAGATGGTGYGATTT	$(A)_{13}$	199 - 215	52	PET	–	–

Notes: Locus ccssr4 and ccssr9 were developed by Chung and Staub (2003) using chloroplast sequences from Nicotiana tabacum L. Sampling location codes: Grand Marais (GM), Petoskey State Park (PS), Traverse City (TC), Good Harbor Bay (GHB), Sleeping Bear Point (SBP), Dune Climb (DC), Dune Plateau (DP), Empire Bluffs (EB), Platte Bay (PB), South Boundary (SB), Zetterberg Preserve (ZP), Arcadia Dunes (AD). [a]Optimal annealing temperature was 62˚C for all loci except for BB_2888, where it was 63 ˚C. [b]Used 2.5 mM MgCl2 per sample to amplify locus.

958
959
960
961

Table 2 Genetic diversity indices for baby's breath from each sampling location at 14 nSSRs and 2 cpSSRs.

	Sampling Locations											
	GM	PS	TC	GHB	SBP	DC	DP	EB	PB	SB	ZP	AD
nSSR Loci												
BB_21680												
N	35	30	30	20	25	23	30	19	20	20	30	30
N_A	3	3	4	3	3	4	3	4	3	4	4	3
H_O	0.286	0.667	0.300	0.450	0.440	0.522	0.500	0.421	0.500	0.400	0.500	0.700
H_E	0.411	0.539	0.534	0.540	0.582	0.481	0.540	0.676	0.524	0.510	0.548	0.546
F_{IS}	**0.3186**	−0.2198	**0.4517**	0.1915	0.2636	−0.0624	0.0909	**0.4000**	0.0709	**0.2400**	0.1040	−0.2661
BB_6627												
N	35	30	30	20	24	23	30	20	20	20	30	30
N_A	2	1	2	2	2	2	2	2	2	2	2	2
H_O	0.086	0.000	0.167	0.500	0.333	0.435	0.500	0.250	0.450	0.550	0.300	0.467
H_E	0.082	0.000	0.153	0.480	0.330	0.499	0.495	0.219	0.489	0.439	0.255	0.464
F_{IS}	−0.0303	–	−0.0741	−0.0160	0.0108	0.1506	0.0068	−0.1176	0.1047	−0.2294	−0.1600	0.0122
BB_3968												
N	35	30	30	20	25	23	30	20	20	20	30	30
N_A	3	2	1	4	3	3	4	4	3	4	3	2
H_O	0.143	0.067	0.000	0.400	0.240	0.304	0.367	0.450	0.550	0.400	0.500	0.133
H_E	0.207	0.064	0.000	0.476	0.246	0.334	0.414	0.475	0.509	0.345	0.418	0.180
F_{IS}	**0.3241**	−0.0175	–	0.1850	0.0432	0.1098	0.1320	0.0782	−0.0556	−0.1343	−0.1805	0.2750
BB_5151												
N	35	29	30	19	25	23	30	19	20	20	30	28
N_A	2	2	2	2	2	2	2	2	2	2	2	2
H_O	0.057	0.034	0.133	0.158	0.200	0.391	0.467	0.526	0.400	0.400	0.200	0.179
H_E	0.056	0.034	0.231	0.494	0.449	0.466	0.491	0.465	0.480	0.375	0.180	0.499
F_{IS}	−0.0149	−0.018	0.4369	**0.6949**	**0.5683**	0.1818	0.0667	−0.1043	0.1915	−0.0411	−0.0943	**0.6530**
BB_4443												
N	35	30	30	20	25	23	30	19	20	19	30	30
N_A	3	5	3	9	9	9^A	9	5	11	7	10^A	5
H_O	0.257	0.800	0.400	0.800	0.640	0.783	0.767	0.842	0.900	0.526	0.667	0.567
H_E	0.338	0.701	0.399	0.808	0.769	0.778	0.758	0.749	0.853	0.593	0.651	0.663
F_{IS}	**0.2537**	−0.1244	0.0156	0.0349	0.1804	0.0161	0.0052	−0.0971	−0.0301	0.2193	−0.0078	0.1623
BB_31555												
N	28	30	30	20	25	23	30	20	20	20	30	30
N_A	1	2	2	3	4	4	4	4	4	4	4	3
H_O	0.000	0.233	0.333	0.650	0.800	0.478	0.600	0.650	0.750	0.500	0.600	0.467
H_E	0.000	0.255	0.278	0.609	0.727	0.650	0.614	0.654	0.745	0.583	0.663	0.545
F_{IS}	–	0.1018	−0.1837	−0.0422	−0.0799	0.2851	0.0396	0.0314	0.0189	0.1667	0.1122	0.1603
BB_14751												
N	34	30	30	20	25	23	30	20	20	20	28	30
N_A	5^A	3	4	7	6	7	8	9	9	10	6	7
H_O	0.676	0.200	0.467	0.650	0.600	0.478	0.633	0.800	0.600	0.650	0.750	0.467
H_E	0.666	0.287	0.548	0.714	0.633	0.618	0.769	0.790	0.621	0.646	0.675	0.762
F_{IS}	**−0.0013**	0.3176	−0.0899	0.1099	0.0722	0.2473	0.1933	0.0130	0.0579	0.0159	−0.0925	0.2632
BB_3335												
N	33	30	30	20	25	23	30	20	20	20	30	30
N_A	5	3	4	8	8	9	7	5	9	10	8	6
H_O	0.242	0.500	0.433	0.800	0.760	0.826	0.667	0.800	0.750	0.850	0.767	0.600
H_E	0.403	0.562	0.369	0.818	0.732	0.827	0.817	0.694	0.808	0.815	0.789	0.709
F_{IS}	**0.4115**	**0.1265**	−0.1564	0.0470	−0.0179	0.0234	**0.2000**	−0.1280	0.0967	−0.0173	0.0451	0.1701

Notes: *N* number of individuals, N_A number of alleles per locus, H_O observed heterozygosity, H_E expected heterozygosity, F_{IS} inbreeding coefficient (Weir and Cockerham 1984), A_R allelic richness for each population averaged across loci, *H* haploid diversity, N_H number of haplotypes for each population averaged across loci, H_R haplotype richness for each population averaged across loci. Bold values indicate loci that deviated from Hardy-Weinberg equilibrium. ^{A} denotes a private allele, ^{P} denotes a private haplotype. Sampling location codes: Grand Marais (GM), Petoskey State Park (PS), Traverse City (TC), Good Harbor Bay (GHB), Sleeping Bear Point (SBP), Dune Climb (DC), Dune Plateau (DP), Empire Bluffs (EB), Platte Bay (PB), South Boundary (SB), Zetterberg Preserve (ZP), Arcadia Dunes (AD).

962
963

Table 2 (Cont) Genetic diversity indices for baby's breath from each sampling location at 14 nSSRs and 2 cpSSRs.

	Sampling Locations											
	GM	PS	TC	GHB	SBP	DC	DP	EB	PB	SB	ZP	AD
nSSR Loci												
BB_4258												
N	35	30	30	20	25	23	30	20	20	20	30	30
N_A	1	1	2	3^A	2	2	2	1	2	4^A	3	2
H_O	0.000	0.000	0.133	0.150	0.240	0.087	0.033	0.000	0.150	0.250	0.400	0.300
H_E	0.000	0.000	0.124	0.141	0.269	0.083	0.033	0.000	0.139	0.228	0.326	0.339
F_{IS}	–	–	−0.0545	−0.0364	0.1273	−0.0233	−0.017	–	−0.0556	−0.0734	−0.2104	0.1329
BB_3913												
N	35	30	30	20	25	23	30	20	20	20	30	30
N_A	3	2	3	4	4	4	4	4	4	4	4	2
H_O	0.171	0.133	0.300	0.400	0.480	0.565	0.667	0.550	0.500	0.550	0.600	0.467
H_E	0.207	0.124	0.292	0.471	0.537	0.619	0.578	0.614	0.494	0.621	0.638	0.444
F_{IS}	0.1873	−0.0545	−0.0166	0.1762	0.1259	0.1090	−0.1373	**0.1292**	0.0130	0.1399	0.0769	−0.0331
BB_2888												
N	35	29	30	20	25	23	30	20	20	20	30	30
N_A	4	2	3	4	6	6	5	6	5	6^A	6	5
H_O	0.657	0.586	0.600	0.800	0.680	0.913	0.833	0.750	0.800	0.800	0.900	0.667
H_E	0.594	0.498	0.651	0.734	0.724	0.772	0.793	0.768	0.746	0.734	0.786	0.589
F_{IS}	−0.0922	−0.1610	0.0953	−0.0648	0.0811	−0.1608	−0.0335	0.0484	−0.0465	−0.0648	−0.1282	−0.1154
BB_5567												
N	35	30	30	20	25	23	30	20	20	20	30	30
N_A	4	3	4	5	3	3	4	3	4	3	5	5
H_O	0.629	0.533	0.567	0.700	0.480	0.609	0.667	0.400	0.550	0.400	0.600	0.767
H_E	0.716	0.613	0.562	0.745	0.614	0.474	0.604	0.374	0.589	0.371	0.613	0.716
F_{IS}	**0.1368**	0.1463	0.0080	0.0859	0.2371	−0.2649	**−0.0872**	−0.0447	0.0913	−0.0519	0.0387	−0.0545
BB_7213												
N	35	30	30	20	25	23	30	20	20	20	30	30
N_A	3	2	3	3	4	3	3	3	3	5	5	3
H_O	0.229	0.367	0.100	0.500	0.640	0.391	0.500	0.400	0.650	0.500	0.633	0.667
H_E	0.359	0.375	0.096	0.434	0.642	0.638	0.565	0.386	0.611	0.499	0.599	0.633
F_{IS}	**0.3754**	0.0392	−0.0235	−0.1276	0.0241	**0.4054**	0.1317	−0.0100	−0.0378	0.0231	−0.0406	−0.0366
BB_8681												
N	35	28	30	20	24	22	30	19	20	20	30	30
N_A	3	3	2	3	3	3	4	2	3	3	4	3
H_O	0.114	0.357	0.333	0.500	0.500	0.136	0.400	0.211	0.250	0.300	0.467	0.600
H_E	0.109	0.523	0.320	0.395	0.469	0.206	0.456	0.188	0.265	0.464	0.502	0.438
F_{IS}	−0.0342	**0.3333**	−0.0247	−0.2418	−0.0455	0.3571	0.1397	−0.0909	0.0821	**0.3753**	0.0866	−0.3558
A_R *across loci*	2.660	2.320	2.540	3.970	3.750	3.920	3.990	3.660	4.070	4.210	4.190	3.120
cpSSR Loci												
ccssr4												
N	35	30	29	20	25	23	30	20	20	20	30	30
N_A	2	1	1	1	1	1	1	1	1	2	2	1
H	0.25	0.00	0.00	0.00	0.00	0.00	0.00	0.00	0.00	0.32	0.50	0.00
ccssr9												
N	35	30	29	20	25	23	30	20	20	20	30	30
N_A	2^A	1	1	1	1	1	1	1	1	2	2	1
H	0.25	0.00	0.00	0.00	0.00	0.00	0.00	0.00	0.00	0.10	0.12	0.00
N_H *across loci*	2^P	1	1	1	1	1	1	1	1	3	3	1
H_R *across loci*	0.991	0	0	0	0	0	0	0	0	2	1.897	0

Notes: *N* number of individuals, N_A number of alleles per locus, H_O observed heterozygosity, H_E expected heterozygosity, F_{IS} inbreeding coefficient (Weir and Cockerham 1984), A_R allelic richness for each population averaged across loci, *H* haploid diversity, N_H number of haplotypes for each population averaged across loci, H_R haplotype richness for each population averaged across loci. Bold values indicate loci that deviated from Hardy-Weinberg equilibrium. ^{A} denotes a private allele, ^{P} denotes a private haplotype. Sampling location codes: Grand Marais (GM), Petoskey State Park (PS), Traverse City (TC), Good Harbor Bay (GHB), Sleeping Bear Point (SBP), Dune Climb (DC), Dune Plateau (DP), Empire Bluffs (EB), Platte Bay (PB), South Boundary (SB), Zetterberg Preserve (ZP), Arcadia Dunes (AD).

966
967
968
969

Table 3 Pairwise F_{ST} values for nSSR data among all sampling locations based on Weir and Cockerham's (1984) estimate. Darker color – increasing F_{ST} value, lighter color – decreasing F_{ST} value.

	GM	PS	TC	GHB	SBP	DC	DP	EB	PB	SB	ZP	AD
GM	–	–	–	–	–	–	–	–	–	–	–	–
PS	0.221	–	–	–	–	–	–	–	–	–	–	–
TC	0.147	0.121	–	–	–	–	–	–	–	–	–	–
GHB	0.264	0.245	0.221	–	–	–	–	–	–	–	–	–
SBP	0.261	0.246	0.230	0.047	–	–	–	–	–	–	–	–
DC	0.321	0.320	0.277	0.063	0.041	–	–	–	–	–	–	–
DP	0.272	0.265	0.246	0.026	0.029	0.025	–	–	–	–	–	–
EB	0.220	0.240	0.175	0.081	0.069	0.093	0.083	–	–	–	–	–
PB	0.290	0.283	0.260	0.062	0.040	0.050	0.050	0.106	–	–	–	–
SB	0.253	0.266	0.207	0.094	0.057	0.077	0.069	0.068	0.066	–	–	–
ZP	0.240	0.238	0.211	0.071	0.040	0.090	0.055	0.071	0.082	0.017	–	–
AD	0.298	0.254	0.231	0.121	0.121	0.137	0.123	0.170	0.128	0.132	0.128	–

Notes: All values significant at $P \leq 0.005$ after FDR correction (Benjamini and Hochberg 1995). Sampling location codes: Grand Marais (GM), Petoskey State Park (PS), Traverse City (TC), Good Harbor Bay (GHB), Sleeping Bear Point (SBP), Dune Climb (DC), Dune Plateau (DP), Empire Bluffs (EB), Platte Bay (PB), South Boundary (SB), Zetterberg Preserve (ZP), Arcadia Dunes (AD).

970
971
972
973
974
975
976
977
978
979
980
981
982
983
984
985
986
987
988
989
990
991
992

FIGURES

Figure 1

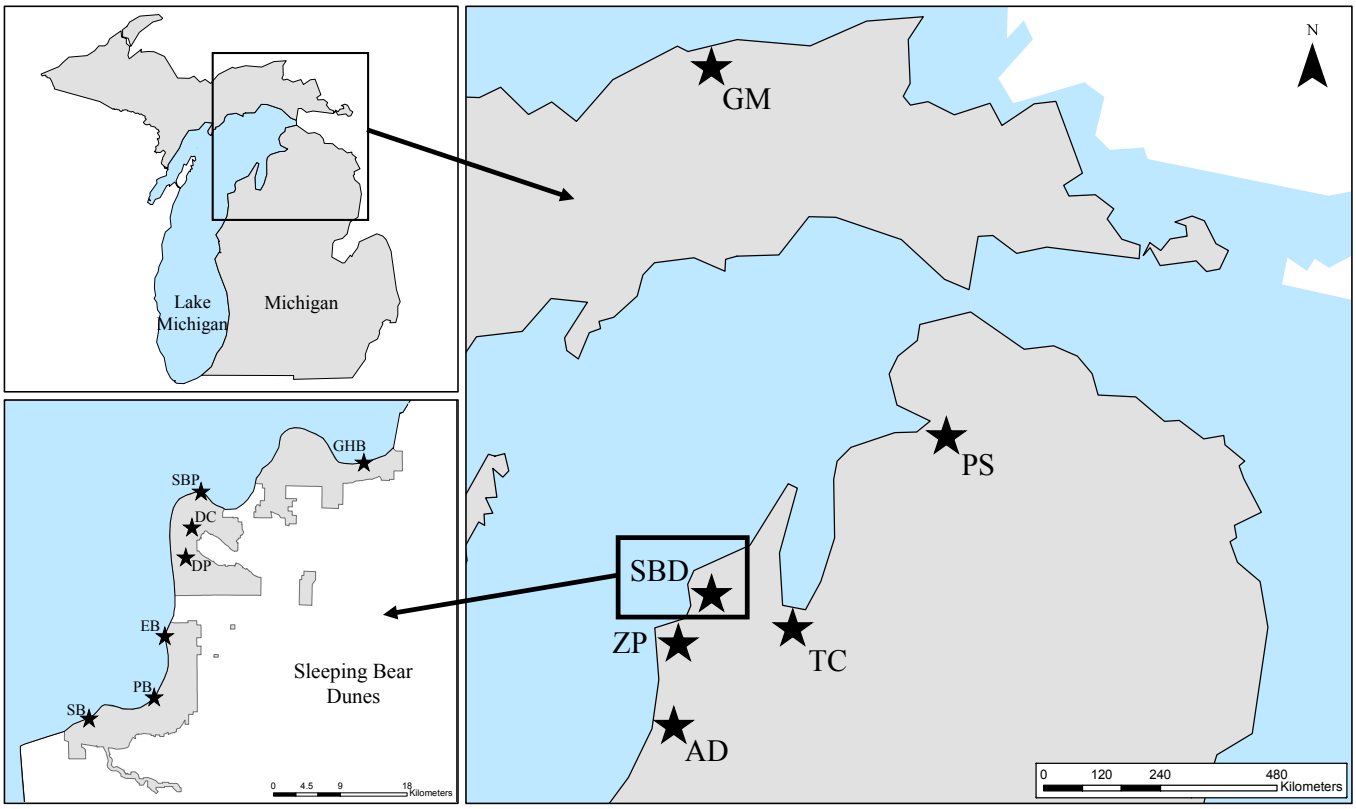

1007

1008

1009 **Figure 2**

1010

1011

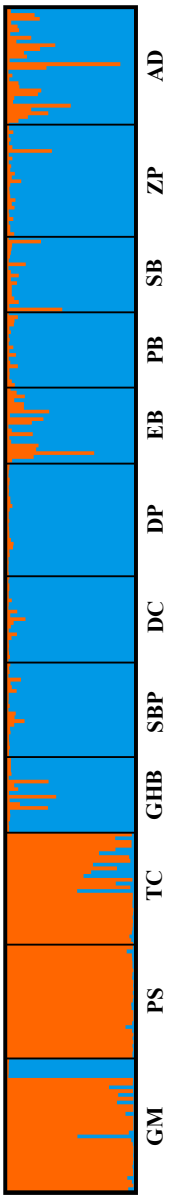

1012

1013

1014 **Figure 3**

1015

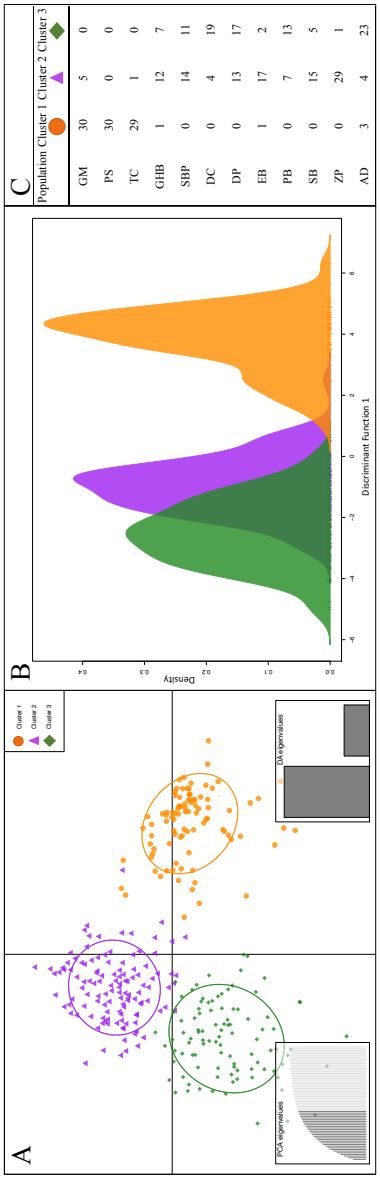

1016

1017

1018

1019

1020

1021

1022

1023 **Figure 4**

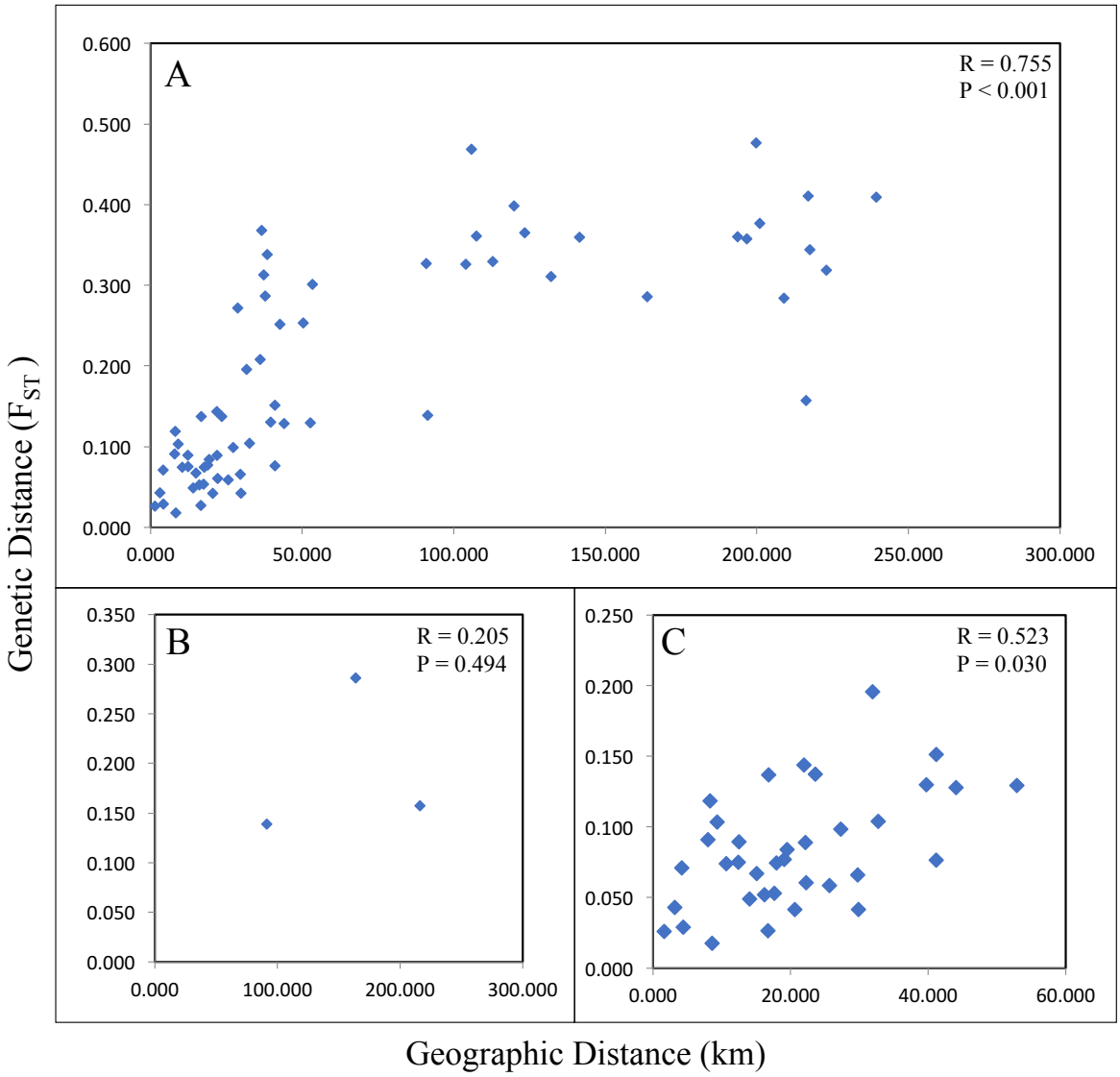

1024

1025

1026

1027

1028

1029

Figure 5

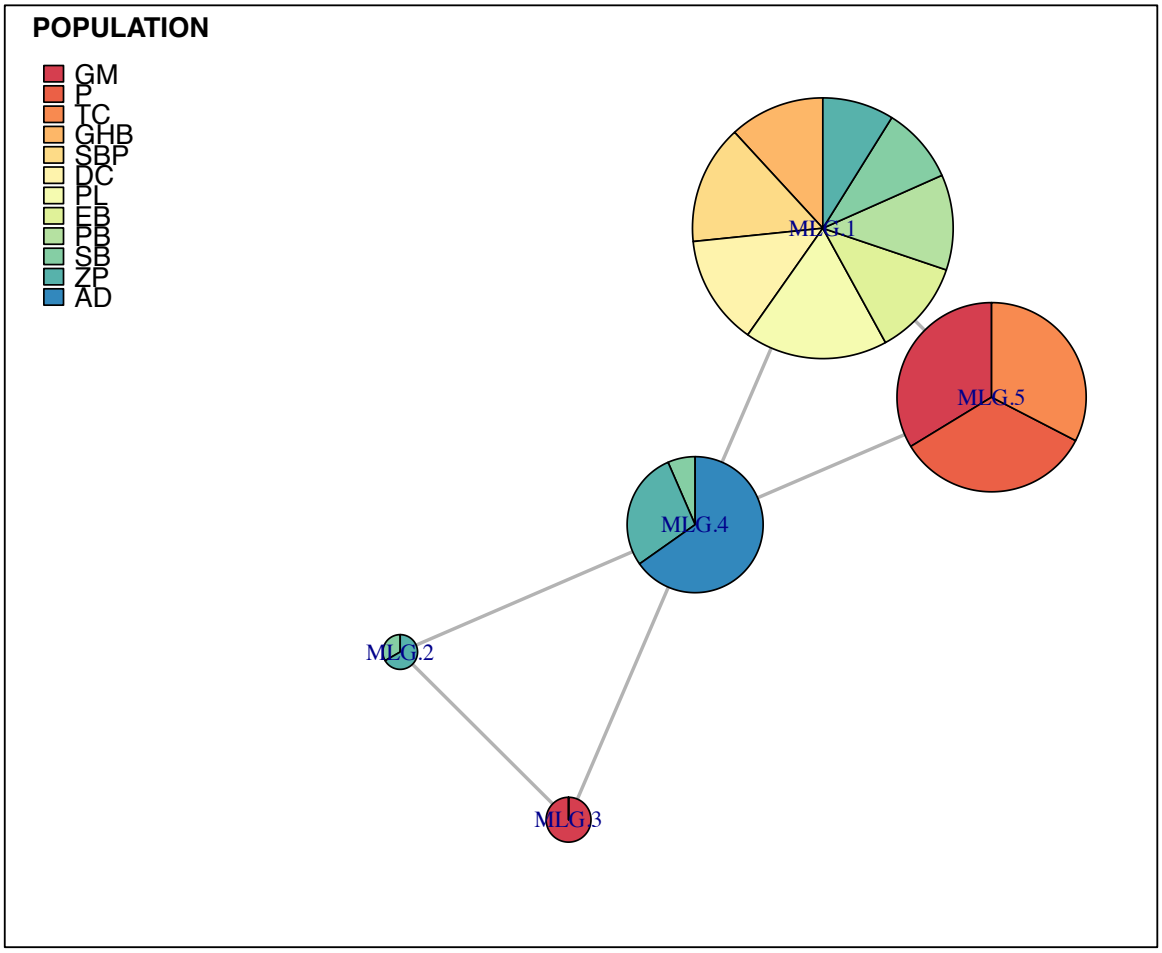

Supplemental A Sampling location names and geographic coordinates for baby's breath analyzed in this study. All locations are in Michigan. Location abbreviations are used in the main text and following tables and figures.

Sampling Location (Code)	*n*	Latitude	Longitude
Grand Marais (GM)	35	46.67825579	-85.97546860
Petoskey State Park (PS)	30	45.40288418	-84.91271857
Traverse City (TC)	30	44.74865647	-85.61882032
Good Harbor Bay (GHB)	20	44.93877954	-85.86802898
Sleeping Bear Point (SBP)	25	44.91095892	-86.04209863
Dune Climb (DC)	23	44.88285396	-86.04280635
Dune Plateau (DP)	30	44.87312491	-86.05846389
Empire Bluff (EB)	20	44.80154168	-86.07121955
Platte Bay (PB)	20	44.73111860	-86.10566158
South Boundary (SB)	20	44.72858265	-86.15892124
Zetterberg Preserve (ZP)	30	44.68665052	-86.25030285
Arcadia Dunes (AD)	30	44.53662395	-86.22527264

Notes: *n* number of individuals sampled.

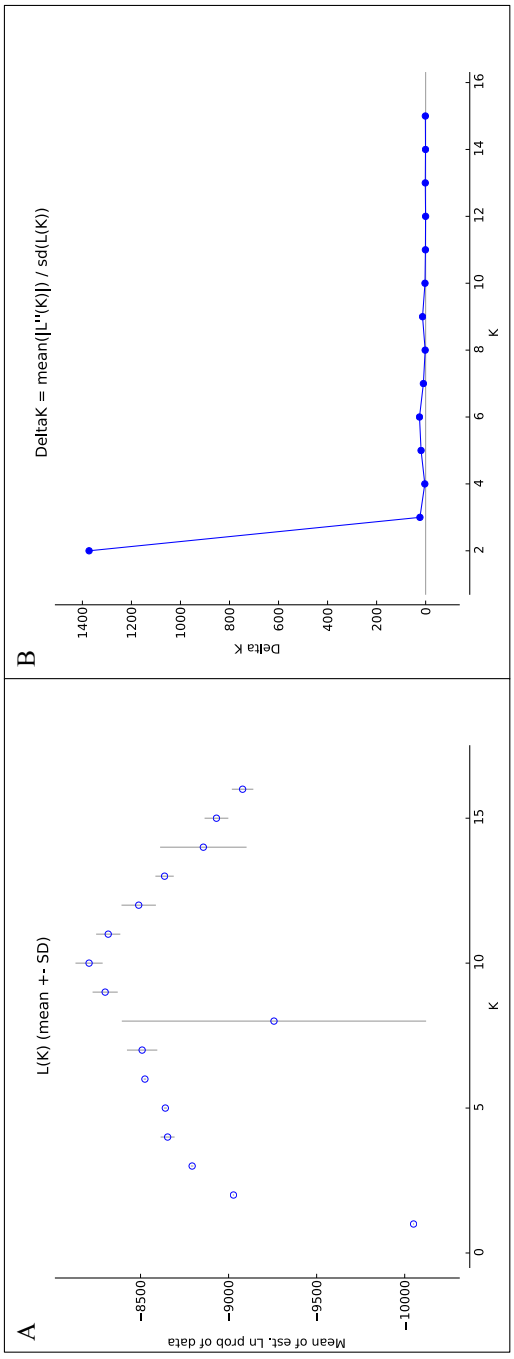

Supplemental B Bayesian clustering analysis of all 12 baby's breath populations from the program STRUCTURE (Pritchard et al. 2000). (A) Mean L(K) (± SD) over 10 runs for each value of *K*. (B) Plot of Evanno's ΔK method (Evanno et al. 2005) where the largest rate of change suggests the highest likelihood of cluster number. This analysis was run without inferring any prior information on sampling location, and two genetic clusters were inferred from this data.

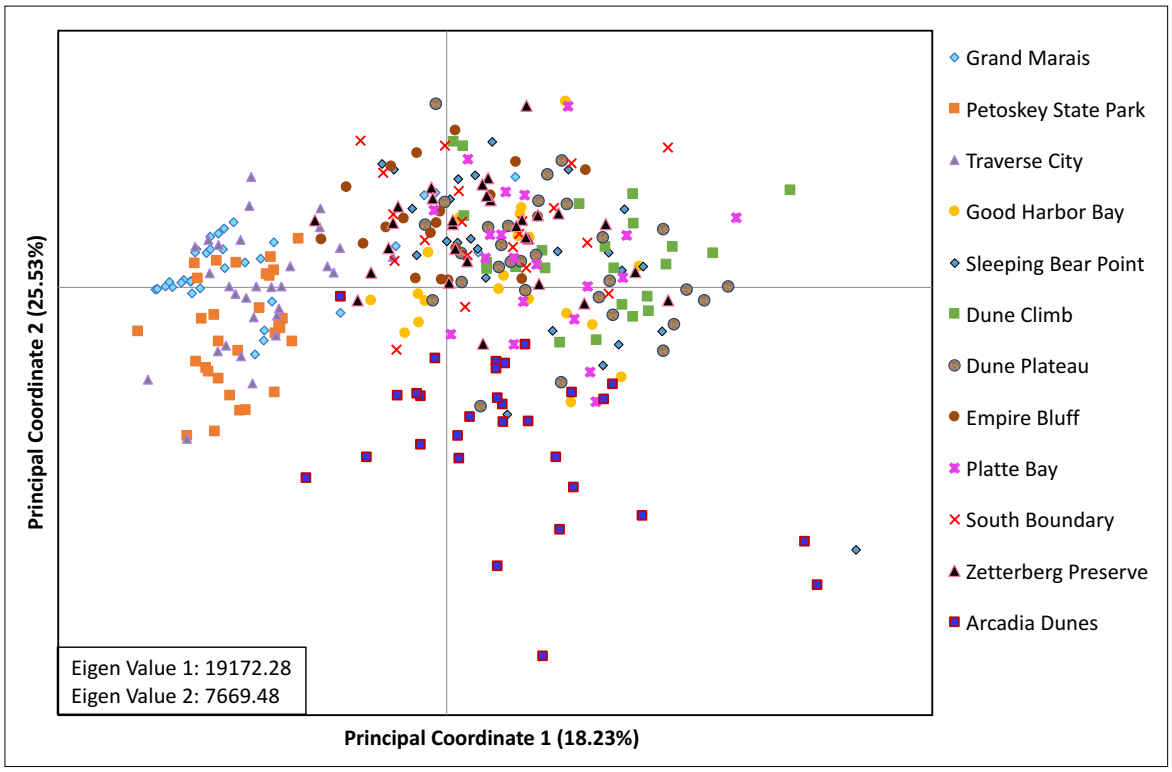

Supplemental C Principal Coordinates Analysis (PCoA) based on a genotypic distance matrix between all baby's breath individuals performed in GenAlEx 6.502 (Peakall and Smouse 2006, 2012). Individuals labeled by sampling location.

1089
1090
1091

Supplemental D Analysis of Molecular Variance (AMOVA) for 14 nuclear and 2 chloroplast SSR loci in 12 populations of baby's breath. Regional differences identified in the Bayesian clustering analysis ($K = 2$) were included in AMOVA, and the analysis was based on **Φ** estimates to compare variance across both marker types following Excoffier et al. (1992) and Weir and Cockerham (1984).

	nSSRs				cpSSRs			
Source of Variation	df	% of Variation	**Φ** – statistics	P – value	df	% of Variation	**Φ** – statistics	P – value
Among regions	1	22.62	0.226	0.0001	1	26.27	0.263	0.0001
Among populations within regions	10	12.89	0.167	0.0001	10	47.37	0.643	0.0001
Within populations	301	64.49	0.355	0.0001	301	26.36	0.736	0.0001

1092
1093
1094